Full characterization of the signal and idler noise figure spectra in single-pumped fiber optical parametric amplifiers

Zhi Tong,[1]* Adonis Bogris,[2] Magnus Karlsson,[1] and Peter A. Andrekson[1]

[1]*Photonics Laboratory, Department of Microtechnology and Nanoscience, Chalmers University of Technology, SE-412 96 Göteborg, Sweden*

[2]*Department of Informatics and Telecommunications, National and Kapodistrian University of Athens, 15784 Athens, Greece*

**zhi.tong@chalmers.se*

Abstract: For the first time, four different noise sources, which are amplified quantum noise, Raman phonon seeded excess noise, pump transferred noise (PTN), and pump residual noise, are considered simultaneously to model the wavelength-dependent noise figure in a single-pumped fiber optical parametric amplifier. An asymmetric signal NF spectrum induced by both Raman phonon seeded excess noise and Raman gain modified PTN is measured in the electrical domain. Theoretical results agree very well with the experimental data. The idler NF spectrum is also analyzed and measured, which shows a more symmetric profile.

OCIS codes: (060.2320) Fiber optics amplifiers and oscillators; (190.4380) Nonlinear optics, four-wave mixing; (190.5650) Raman effect.

References and links

1. J. Hansryd, P. A. Andrekson, M. Westlund, J. Lie, and P.-O. Hedekvist, "Fiber-based optical parametric amplifiers and their applications," IEEE J. Sel. Top. Quantum Electron. **8**(3), 506–520 (2002).
2. Y. Yamamoto, and K. Inoue, "Noise in amplifiers," J. Lightwave Technol. **21**(11), 2895–2915 (2003).
3. P. Kylemark, P.-O. Hedekvist, H. Sunnerud, M. Karlsson, and P. A. Andrekson, "Noise characteristics of fiber optical parametric amplifiers," J. Lightwave Technol. **22**(2), 409–416 (2004).
4. P. L. Voss, and P. Kumar, "Raman-noise-induced noise-figure limit for $\chi^{(3)}$ parametric amplifiers," Opt. Lett. **29**(5), 445–447 (2004).
5. P. L. Voss, and P. Kumar, "Raman-effect induced noise limits on $\chi^{(3)}$ parametric amplifiers and wavelength converters," J. Opt. B Quantum Semiclassical Opt. **6**(8), 762–770 (2004).
6. R. Tang, P. L. Voss, J. Lasri, P. Devgan, and P. Kumar, "Noise-figure limit of fiber-optical parametric amplifiers and wavelength converters: experimental investigation," Opt. Lett. **29**(20), 2372–2374 (2004).
7. A. Durécu-Legrand, C. Simonneau, D. Bayart, A. Mussot, T. Sylvestre, E. Lantz, and H. Maillotte, "Impact of pump OSNR on noise figure for fiber optical parametric amplifiers," IEEE Photon. Technol. Lett. **17**(6), 1178–1180 (2005).
8. P. Kylemark, M. Karlsson, and P. A. Andrekson, "Gain and wavelength dependence of the noise-figure in fiber optical parametric amplifiers," IEEE Photon. Technol. Lett. **18**(11), 1255–1257 (2006).
9. A. Bogris, D. Syvridis, P. Kylemark, and P. A. Andrekson, "Noise characteristics of dual-pump fiber-optic parametric amplifiers," J. Lightwave Technol. **23**(9), 2788–2795 (2005).
10. J. L. Blows, and S. E. French, "Low-noise-figure optical parametric amplifier with a continuous-wave frequency-modulated pump," Opt. Lett. **27**(7), 491–493 (2002).
11. P. Kylemark, and M. Marhic, "Quantum-limited amplification in a fiber optical parametric amplifier," in *European Conference on Optical Communications*, paper Tu. 3.B.3 (2008).
12. R. H. Stolen, J. P. Gordon, W. J. Tomlinson, and H. A. Haus, "Raman response function of silicon-core fibers," J. Opt. Soc. Am. B **6**(6), 1159–1166 (1989).
13. G. P. Agrawal, *Nonlinear fiber optics* (Academic, 1995), Chap. 8.
14. N. A. Olsson, "Lightwave systems with optical amplifiers," J. Lightwave Technol. **7**(7), 1071–1082 (1989).
15. C. J. McKinstrie, M. Yu, M. G. Raymer, and S. Radic, "Quantum noise properties of parametric processes," Opt. Express **13**(13), 4986–5012 (2005), http://www.opticsinfobase.org/oe/abstract.cfm?URI=oe-13-13-4986.
16. L. Boivin, F. X. Kärtner, and H. A. Haus, "Analytical solution to the quantum field theory of self-phase modulation with a finite response time," Phys. Rev. Lett. **73**(2), 240–243 (1994).
17. Z. Tong, A. Bogris, M. Karlsson and P. A. Andrekson, "Raman induced asymmetric pump noise transfer in fiber optical parametric amplifiers," to appear in IEEE Photon. Technol. Lett..
18. G. P. Agrawal, *Fiber-Optic Communications Systems* (New York: John Wiley & Sons, 2002), Chap. 6.

#118960 - $15.00 USD Received 26 Oct 2009; revised 10 Dec 2009; accepted 12 Jan 2010; published 27 Jan 2010

19. M. E. Marhic, G. Kalogerakis, K. K. Y. Wong, and L. G. Kazovsky, "Pump-to-signal transfer of low-frequency intensity modulation in fiber optical parametric amplifiers," J. Lightwave Technol. **23**(3), 1049–1055 (2005).
20. M. Movassaghi, M. K. Jackson, V. M. Smith, and W. J. Hallam, "Noise figure of erbium-doped fiber amplifiers in saturated operation," J. Lightwave Technol. **16**(5), 1461–1465 (1998).
21. P. Velanas, A. Bogris, and D. Syvridis, "Impact of dispersion fluctuations on the noise properties of fiber optical parametric amplifiers," J. Lightwave Technol. **24**(5), 2171–2178 (2006).

1. Introduction

Fiber optical parametric amplifiers (FOPAs) have many unique characteristics such as uni-directional amplification, simultaneous conjugated idler generation, ultrafast response and noiseless amplification in phase-sensitive mode, which make them potential candidates for future ultra-low noise amplification as well as for all-optical signal processing [1]. In theory, 3 dB quantum-limited noise figure (NF) can be reached in a phase-insensitive (PI) FOPA, since there is no stimulated absorption in parametric amplification compared to EDFAs, and only vacuum quantum noise is amplified [2]. However, in practice other noise sources exist in FOPAs which make the quantum-limit difficult to achieve.

To date, four different noise mechanisms in a practical PI-FOPA have been reported separately, which are amplified quantum noise (AQN) [3], Raman phonon seeded excess noise [4–6], pump transferred noise (PTN) [3,7–9] and residual pump noise [10], respectively. Among them, AQN is the fundamental noise mechanism, and the others can be treated as excess noise sources. AQN originates from the amplification of the vacuum quantum fluctuation and leads to the well-known 3 dB quantum limit. Raman phonon seeded excess noise comes from the delayed nonlinear response in optical fibers, which couples thermal phonons and adds noise to both Stokes and anti-Stokes waves. PTN is caused by the ultrafast response of the parametric process, which turns pump intensity noise into signal power fluctuation instantaneously. Last but not least, residual pump noise, due to the imperfect pump filtering, makes a part of pump noise (mainly from the pump booster) leak out and then combine with the signal at the input of the amplifier. In most experimental setups, highly-nonlinear fibers (HNLF) as well as high power EDFA boosters are used to provide efficient parametric amplification. However, HNLFs usually have large Raman gain coefficients, and EDFA boosters unavoidably generate amplified spontaneous emission (ASE). As a result the second and the third noise contributions are not trivial in many cases, and sometimes they may dominate the noise performance. In addition, although pump residual noise can be effectively suppressed by high-quality narrow-band filters, in some conditions (e.g. using high output pump power, very low signal input or very small signal-to-pump wavelength separation, etc.), it may significantly degrade the signal noise performance.

To date, all the published investigations focused only on one specific excess noise contribution (apart from AQN) in the FOPA, which may lead to inconsistent conclusions when compared to the experimental results. For example, in Ref [8], only PTN was theoretically studied while both PTN and Raman phonon seeded excess noise were measured (in the electrical domain), however, good agreement between theory and experiment can still be derived, which was not adequately explained. Moreover, it has been recognized that the true NF of FOPAs can only be measured in the electrical domain, because of the narrow-band nature of PTN [8]. However, only a few electrically measured NF results have been reported, and actually no accurate NF measurements for either signal or idler wave have been demonstrated over the whole parametric optical gain spectrum (the measurement error in [10] was about ± 2 dB). In Ref [11], the authors demonstrated a quantum-limited NF measurement in a FOPA through suppressing the Raman phonon induced noise. However they measured the NF in the optical domain and thus neglected the PTN. As a result, the full NF spectrum of a PI-FOPA is still not fully evaluated, and how to model the actual NF and which noise contribution is most important in practical FOPAs remain unanswered to date. Answers to these questions would be helpful for a better understanding of the noise performance of phase-insensitive FOPAs.

Motivated by the above issues, in this paper we take into account the four noise contributions simultaneously to analyze the wavelength-dependent NF characteristics for the

#118960 - $15.00 USD Received 26 Oct 2009; revised 10 Dec 2009; accepted 12 Jan 2010; published 27 Jan 2010

first time. An asymmetric signal NF spectrum is observed both theoretically and experimentally, which is due not only to Raman phonon seeded excess noise [4–6] but also to the asymmetric PTN caused by Raman gain. Moreover, the NF spectrum of the wavelength converted idler is also analyzed and measured, the results of which show a more symmetric NF profile compared with the amplified signal. Very good agreement is obtained between theory and electrical measurements, which proves that the noise performance of both signal and idler in a PI-FOPA is determined by these combined noise contributions.

2. Theoretical model

In this paper, we only focus on the conventional NF defined in the linear (non-saturated) regime. By assuming un-depleted pump as well as co-polarization amplification, and considering Raman effect (no Raman coupled phonons are introduced), we have [5,12,13]

$$\frac{d}{dz}\begin{bmatrix} A_a \\ A_s^* \end{bmatrix} = \begin{bmatrix} j\{[\dfrac{H(\Omega)+H^*(-\Omega)}{2}]P_P - \dfrac{\Delta\beta}{2}\} & jH(\Omega)P_P \\ -jH^*(-\Omega)P_P & -j\{[\dfrac{H(\Omega)+H^*(-\Omega)}{2}]P_P - \dfrac{\Delta\beta}{2}\} \end{bmatrix} \begin{bmatrix} A_a \\ A_s^* \end{bmatrix} = \mathbf{G}\cdot\begin{bmatrix} A_a \\ A_s^* \end{bmatrix}. \quad (1)$$

where $A_{a,\,s}$ represent the complex field amplitudes of anti-Stokes and Stokes waves, P_P is the launched pump power, subscript * represents conjugation operation and $H(\Omega) = \gamma[1 - f + fF_R(\Omega)]$. $F_R(\Omega)$ is the complex Raman susceptibility, γ is the fiber nonlinearity, f accounts for the fractional contribution of the Raman to the total nonlinearity (for silica fiber we use $f = 0.18$ here [12]), and Ω is the frequency shift between the pump and Stokes (or anti-Stokes) waves. The imaginary part of $F_R(\Omega)$ is the Raman gain coefficient, which can be measured directly, while the real part can be obtained from the Kramers-Krönig relation [12]. The phase mismatch is denoted as $\Delta\beta = 2\beta_P - \beta_a - \beta_s$, where $\beta_{P,a,s}$ represent the linear propagation constants at pump, anti-Stokes and Stokes wavelengths, respectively. Based on the matrix exponential, Eq. (1) has an analytical solution as

$$\begin{bmatrix} A_a(z) \\ A_s^*(z) \end{bmatrix} = \exp(\mathbf{G}z)\cdot\begin{bmatrix} A_a(0) \\ A_s^*(0) \end{bmatrix} = \mathbf{T}\cdot\begin{bmatrix} A_a(0) \\ A_s^*(0) \end{bmatrix}, \quad (2)$$

where either $A_a(0)$ or $A_s(0)$ equals 0 to account for the idler wave in a PI case, and

$$\mathbf{T} = \begin{bmatrix} T_{11} & T_{12} \\ T_{21} & T_{22} \end{bmatrix} = \begin{bmatrix} \cosh(gz) + j\dfrac{k}{2g}\sinh(gz) & j\dfrac{H(\Omega)P_P}{g}\sinh(gz) \\ -j\dfrac{H^*(-\Omega)P_P}{g}\sinh(gz) & \cosh(gz) - j\dfrac{k}{2g}\sinh(gz) \end{bmatrix}, \quad (3)$$

where $k = [H(\Omega) + H^*(-\Omega)]P_P - \Delta\beta$, and $g^2 = H(\Omega)H^*(-\Omega)P_P^2 - k^2/4$. Based on the above equations, the parametric gain as well as wavelength conversion efficiency combined with Raman effect can be obtained.

2.1 Amplified quantum noise

In PI-FOPAs, the vacuum fluctuations at the signal and idler frequencies will be amplified and added to each other, which can be understood from Eq. (2). We have [3,14,15]

$$NF_{sig,AQN} = 2 - 1/G_{sig} \text{ and } NF_{i,AQN} = 2 + 1/G_i, \quad (4)$$

where subscripts *sig* and *i* represent the signal (parametric amplification) and idler (wavelength conversion) waves, which are determined by the input condition, and different from the previous subscripts *a* and *s* accounting for shorter and longer wavelength bands.

#118960 - $15.00 USD Received 26 Oct 2009; revised 10 Dec 2009; accepted 12 Jan 2010; published 27 Jan 2010

According to Eq. (3), $G_{sig} = |T_{11}|^2 = 1 + \gamma^2 P_P^2 \sinh^2(gz)/g^2$ and $G_i = |T_{12}|^2$ is the signal and idler gain, respectively. Equation (4) is the well-known quantum limited NF, which is the inherent noise mechanism in a phase-insensitive optical amplifier. It should be noted that when G_{sig} is less than 0 dB, Eq. (4) is not valid.

2.2 Raman phonon seeded excess noise

According to [16], excess noise will be introduced when considering the finite response time of the nonlinear medium, which is the physics behind the Raman phonon seeded excess noise. Based on the quantum theory, Voss *et. al* have derived formulas of the excess signal NF caused by Raman effects in linear gain regime [4,5] as

$$\begin{aligned} \Delta NF_{Raman,a} &= 1 + [|T_{12}|^2 + (1+2n_{th})\left||T_{11}|^2 - |T_{12}|^2 - 1\right|]/|T_{11}|^2 - NF_{AQN,a}, \text{ or} \\ \Delta NF_{Raman,s} &= 1 + [|T_{21}|^2 + (1+2n_{th})\left||T_{22}|^2 - |T_{21}|^2 - 1\right|]/|T_{22}|^2 - NF_{AQN,s}, \end{aligned} \tag{5}$$

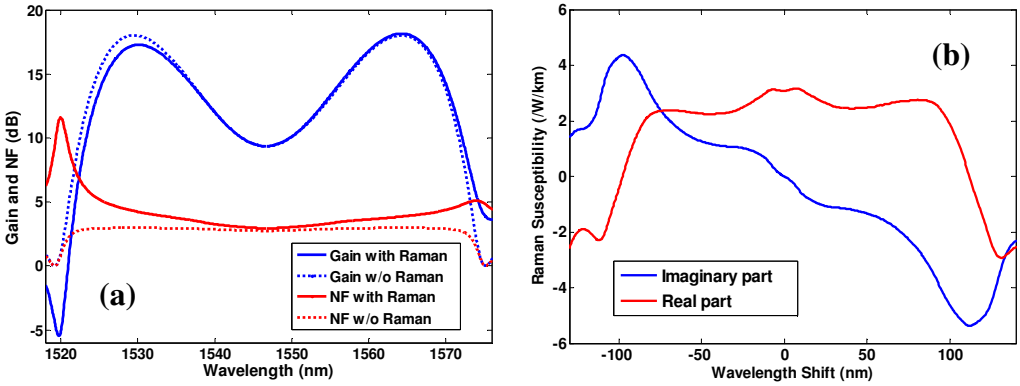

Fig. 1. a) Calculated signal gain and NF spectra with or without Raman effect, and b) the real and imaginary parts of the Raman susceptibility of the HNLF used in the experiments. Pump wavelength is 1546.7 nm.

where subscripts *a* and *s* represent anti-Stokes and Stokes waves, respectively, as used in Eq. (1). The mean phonon number in thermal equilibrium is expressed by $n_{th} = [\exp(h\Omega/(2\pi kT) - 1]^{-1}$. We can also derive the idler NF expression accounting for the wavelength conversion process [5]. Though the gain variations caused by Raman power transfer are not large around the peak gain, the Raman induced additional NF can be significant, especially at the gain edges [4–6] or when high pump power and large gain bandwidth are considered. In Fig. 1, calculated signal gain and NF spectra are compared with or without considering Raman effect, when 250 m HNLF (parameters are λ_0 = 1542 nm, γ = 11.7 $W^{-1}km^{-1}$, α = 0.8 dB/km, and S_0 = 0.019 ps/nm^2·km, obtained from the real HNLF in our experiments) and 0.95 W pump power are used. Both the real and the imaginary parts of $F_R(\Omega)$ of the HNLF used in our experiments are shown in Fig. 1(b), and an eight times larger peak Raman gain coefficient can be observed compared to a conventional dispersion shifted fiber. A clear gain asymmetry can be found at the gain edges, and a larger than 5 dB Raman induced attenuation is shown at the anti-Stokes band. Accordingly, a sharp NF increase is appearing around the gain edge at the shorter wavelength band. Even around the peak gain the average NF is still larger than 4.5 dB. Compared with the parametric amplification, the impacts of Raman effects on the efficiency and NF spectra of the wavelength conversion (idler) are more symmetric, as shown in Fig. 2. The reason is that the conversion efficiency difference between the Stokes and anti-Stokes waves is actually compensated through the asymmetric signal gain.

#118960 - $15.00 USD Received 26 Oct 2009; revised 10 Dec 2009; accepted 12 Jan 2010; published 27 Jan 2010

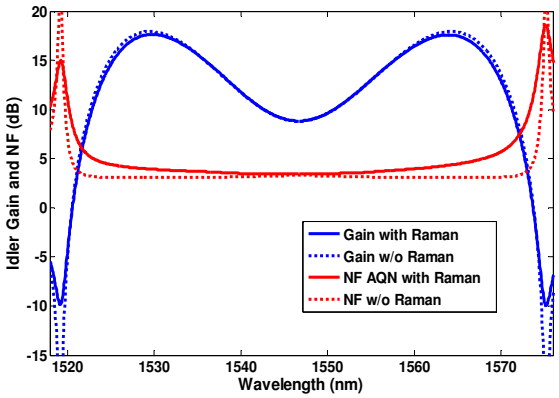

Fig. 2. Calculated idler gain and NF spectra with or without the Raman effect.

2.3 Pump transferred noise

Raman phonon seeded excess noise can to some extent explain why the minimum measured NF in a PI-FOPA cannot reach the quantum limit. However, it cannot explain the signal-power-dependent NF, which was experimentally observed in [7]. Actually, another noise source, i.e. pump transferred noise, causes to this phenomenon, and it has been shown in [8,9] that the PTN is related to the derivative of the gain with respect to pump power, as a first-order approximation. However, in [8,9] no Raman effects were considered. In fact, Raman power transfer will modify the PTN spectrum and make it asymmetric [17]. The NF increase due to PTN combined with Raman gain can be expressed as

$$\Delta NF_{\mathrm{PTN,j}} = P_{in}(\frac{\partial G_j}{\partial P_P})^2 P_P^2 / (OSNR \cdot G_j^2 \cdot h\nu\Delta\nu), \tag{6}$$

where subscript j = *a, s* representing the anti-Stokes or Stokes wave, P_{in} is the input signal power, *OSNR* is the input pump optical signal-to-noise ratio, Δν is the 0.1 nm resolution bandwidth of the OSNR measurement. It should be pointed out that we can also use pump electrical SNR (ESNR) to evaluate pump intensity noise, which has the $ESNR = OSNR/2$ relation when considering identical optical and electrical noise bandwidth and assuming signal beat noise dominating [18]. Actually, pump ESNR measured in the electrical domain is more reliable since it can precisely show the contribution of the intensity noise, while the OSNR measured through noise interpolation might give an inaccurate result when phase noise becomes significant. A good example is that the measured pump ESNR in a FOPA will stay constant along the FOPA whereas the measured OSNR decreases quadractically, as mentioned in [17,19]. As a result, through out this paper we will use pump ESNR to evaluate PTN, which is determined by the relative intensity noise (RIN) of the pump laser as well as the NF of the EDFA booster.

Equation (8) indicates PTN is proportional to $(\partial G_j / \partial P_P)^2$, so a modified PTN spectrum can be expected due to the asymmetric Raman power transfer. Both gain and NF spectra (considering both AQN and PTN) with or without Raman effect are calculated and compared in Fig. 3, which clearly confirms that Raman power transfer will make the PTN spectrum asymmetric. According to Fig. 3(a), larger NF can be observed at the anti-Stokes band, especially at the gain edge, which originates from a larger $\partial G_a / \partial P_P$ caused by Raman power transfer from the anti-Stokes to the Stokes wave. In addition, the NF dependence on the input signal power comes from the P_{in} term in Eq. (6), which is due to the nonlinear relationship between the signal input power and the PTN [8]. This Raman induced tilted PTN, combined with Raman phonon seeded excess noise, will contribute to an asymmetric NF spectrum of a

#118960 - $15.00 USD Received 26 Oct 2009; revised 10 Dec 2009; accepted 12 Jan 2010; published 27 Jan 2010

single-pumped FOPA, and the asymmetry will be even more significant when broadband gain (>100nm) is realized. On the contrary, the PTN spectrum of the wavelength conversion process is almost unchanged after introducing the Raman effect, as shown in Fig. 3(b).

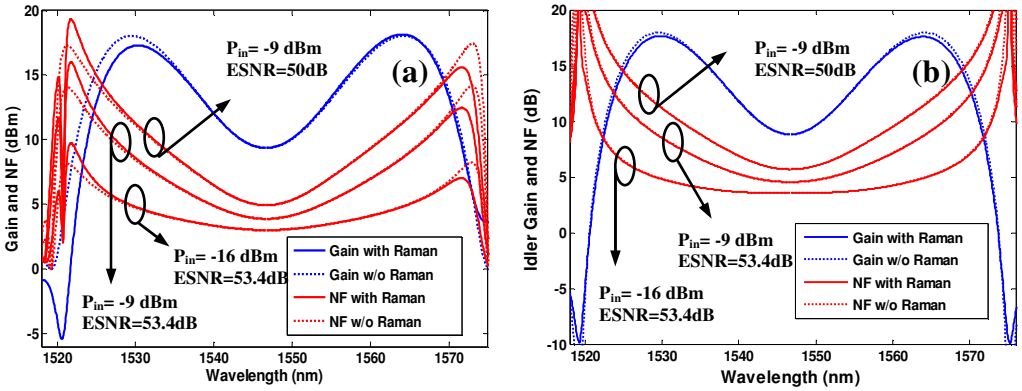

Fig. 3. Calculated a) signal and b) idler gain and NF spectra (AQN + PTN) with or without considering Raman effect.

2.4 Pump residual noise

High power EDFA pump boosters will generate large amount of ASE noise, and in some cases the total ASE power can be comparable to the signal power. For inadequate pump filtering, very high booster gain or small signal-pump wavelength separation, a large amount of residual pump ASE will be added to the input signal, and then amplified simultaneously to degrade the output noise performance. It should be noted that the residual pump noise at the idler wavelength will also be amplified and copied to the signal. Accordingly we can obtain the following equation to model the additional NF induced by pump residual noise:

$$\Delta NF_{res} = \frac{2(G_s - 1)(S_{ASE\_Signal} + S_{ASE\_Idler}) \cdot P(\lambda)}{G_s h v_s}, \qquad (7)$$

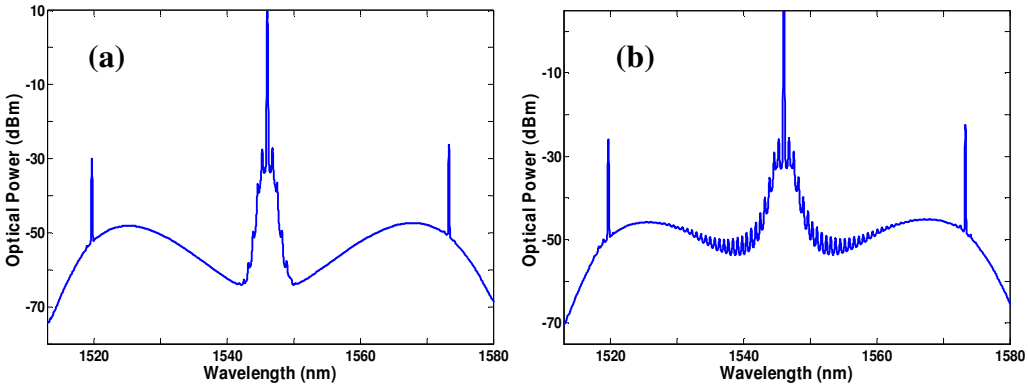

Fig. 4. Measured output optical spectrum of a single-pumped FOPA with (a) two cascaded pump filters and (b) only one pump filter. The resolution bandwidth is 0.5 nm.

where S_{ASE_Signal} and S_{ASE_Idler} represent the ASE power spectral densities (at the output of the EDFA booster) at the signal and idler wavelengths, respectively, which can be measured via an optical spectrum analyzer, and $P(\lambda)$ is the transmission response of the pump filter. Equation (7) is also applied to the wavelength conversion case. In Fig. 4, we compare the

#118960 - $15.00 USD Received 26 Oct 2009; revised 10 Dec 2009; accepted 12 Jan 2010; published 27 Jan 2010

measured output optical spectra of a single-pumped FOPA with only one and two-cascaded pump filters. An obvious pump residual side-mode amplification can be noticed when only one pump filter is used, which makes the optical spectrum quite noisy. The impact of the pump residual ASE on signal NF will be experimentally demonstrated in the next section.

3. Experimental results and discussion

Based on the results of section 2, we can achieve the total signal or idler NF of a PI-FOPA as

$$NF_{total} = NF_{AQN} + \Delta NF_{Raman} + \Delta NF_{PTN} + \Delta NF_{res}. \quad (8)$$

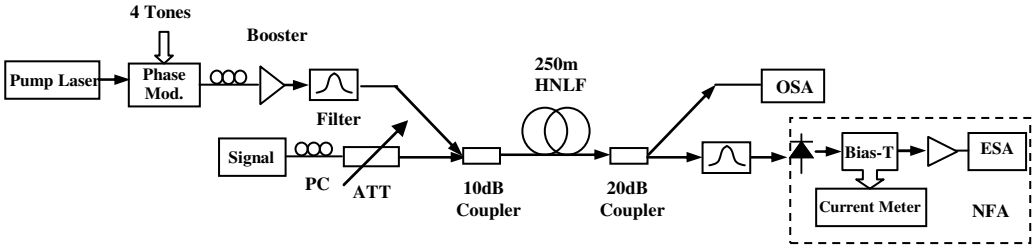

Fig. 5. Measurement setup. NFA: Noise figure analyzer; ESA: Electrical spectrum analyzer; OSA: Optical spectrum analyzer; PC: Polarization controller; ATT: Variable attenuator.

Next we will experimentally verify this combined noise model. In Fig. 5 the experimental setup is demonstrated. A 20 mW output DFB laser (1546.7 nm) was used as the pump laser, which was phase-modulated by four tones (100, 300, 900 and 2700 MHz) to suppress stimulated Brillouin scattering. After a high power EDFA booster, the amplified pump was filtered and combined with signal by a 10 dB coupler. A 250 m HNLF were used as the gain medium. Finally the amplified signal was filtered and detected by the NF analyzer. The detected signal and noise components were separated by a bias-T, and then measured by a current meter and electrical spectrum analyzer, respectively. It should be noted that a high-efficiency photodetector as well as a low-noise RF-amplifier is important for good accuracy. After carrying out calibration for shot noise and subtracting laser RIN noise [20], accurate NF and ESNR can be measured in the electrical domain even for low gain. We choose 874.6 MHz as the central frequency to measure noise level, with 2 MHz resolution bandwidth and 3 Hz video bandwidth. In most cases, the NF measurement error is within ± 0.35 dB. The bandwidth of the FOPA in the experiment is mainly limited by our measurement capability of the NF spectrum, since we want to measure the NF spectrum covering the whole gain band.

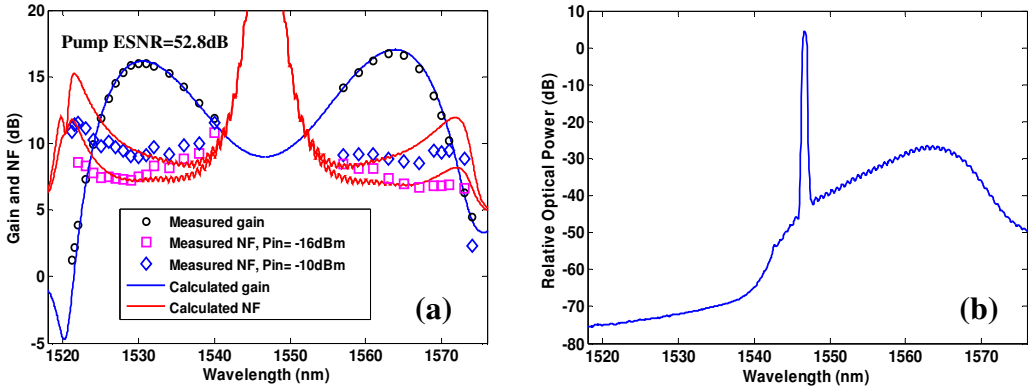

Fig. 6. a) Comparison of the calculated and measured signal gain and NF spectra with only one pump filter (2 nm 3-dB bandwidth), 0.95 W pump launched power is used in calculation, and b) the filtered ASE spectrum of the booster.

#118960 - $15.00 USD Received 26 Oct 2009; revised 10 Dec 2009; accepted 12 Jan 2010; published 27 Jan 2010

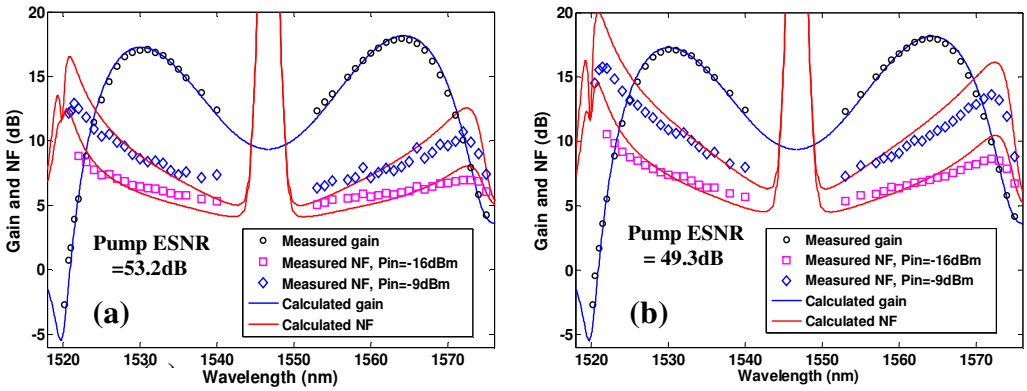

Fig. 7. Comparison of the calculated and the measured signal gain and NF spectra with two cascaded pump filters (1 nm 3-dB bandwidth), with a) 53.2 dB and b) 49.3 dB launched pump ESNR. A 0.95 W pump power was used.

The measured and calculated signal gain and NF spectra with only one pump filter (3 dB bandwidth of 2 nm) are shown in Fig. 6(a), and the output EDFA ASE spectrum is shown in Fig. 6(b). The vertical size of the NF marker is of the order of the measurement error. Only two fitting parameters were used in the calculation, i.e. P_P = 0.9 W and $\beta_4 = 2 \times 10^{-55}$ s^4/m, and other parameters are directly achieved from the measured data. The transmission response of the pump filter was measured as $P(\lambda) = B_f^2 / [(\lambda_s - \lambda_0)^4 + B_f^2]$, where λ_0 is the pump central wavelength, and B_f indicates half the 3 dB filter bandwidth. Very good agreement between calculated and measured gain/NF spectra is observed, and an NF increase due to pump residual noise is observed for wavelengths close to the pump. The gain profile remains the same at different signal input levels, which confirms the linear operation regime. A 3 dB Raman induced attenuation at the anti-Stokes band was measured around 1520 nm. In Fig. 7, we show measured and calculated NF and gain spectra with two cascaded filters (1st filter: 2 nm bandwidth, and the 2nd filter: 0.2 nm bandwidth) to effectively suppress the pump residual noise, and still very good agreement can be achieved at 53.2 dB and 49.3 dB pump ESNR, respectively, which confirms our theoretical model further. The pump ESNR is controlled by changing the input power to the booster, while keeping the booster output constant. Comparing Fig. 6 and 7, a significant NF increase within ± 10 nm range around pump wavelength can be observed in Fig. 6, which is clearly due to the pump residual ASE noise. This result indicates that pump filters with high selectivity must be used to minimize such impact, and only considering PTN + Raman phonon induced noise is not enough to get a satisfying agreement between theory and experiment when the signal-to-pump wavelength separation is small or the isolation of the pump filter is inadequate. In addition, signal-input- and pump-SNR-dependent, asymmetric NF spectra have been shown in Fig. 7 as expected, and the relatively high NFs are mainly due to the combined Raman induced noise and PTN. The deviation between the calculated and measured NF spectra may be attributed to 1) polarization misalignment between signal and pump waves, due to polarization mode dispersion and nonlinear polarization rotation (which is not significant here since the HNLF we used has a PMD value less than 0.04 $ps/\sqrt{km}$), and 2) zero-dispersion-wavelength fluctuations induced gain spectrum distortion, which can smear out the sharp gain decrease and thus reduce the NF at the gain edges to some degree [21]. Even though the calculated and measured gain spectra are similar, the NF deviation still appears since we used β_4 as a fitting parameter to match the calculated gain spectrum to the experiment, which modifies the gain band slightly but does not have the same impacts on NF as the ZDW fluctuations do. For a properly designed FOPA with low noise pump and low input signal, Raman phonon seeded noise will dominate at larger pump-signal separation, while pump residual ASE will dominate the region close to the pump wavelength. However, if one increases the input signal power or

#118960 - $15.00 USD Received 26 Oct 2009; revised 10 Dec 2009; accepted 12 Jan 2010; published 27 Jan 2010

degrade the pump SNR, PTN will become larger and finally dominant. In Ref [8], the PTN contribution was actually larger than the Raman induced noise since a pump laser with relatively low SNR was used, thus only considering PTN could still give a good prediction.

Finally, the idler gain and NF spectra are also calculated and measured by taking into account all the noise contributions, as shown in Fig. 8. For comparison, we choose the same configuration as used in Fig. 7(a). Due to the idler gain measurement uncertainty by using an OSA, slightly larger NF error is obtained. According to Fig. 8, a more symmetric NF spectrum can be observed for the wavelength conversion process at different input signal levels, which confirms the previous theoretical analysis. The measured results agree with theory quite well, both with respect to gain and NF.

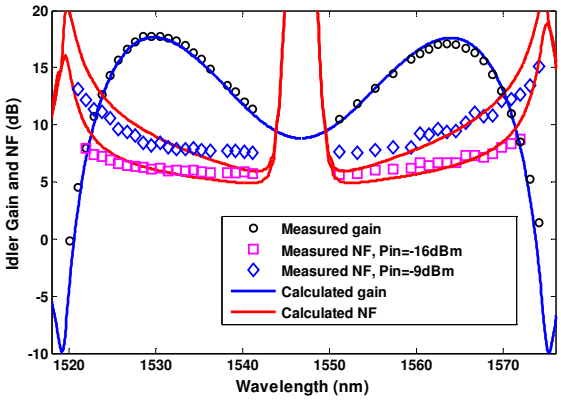

Fig. 8. Comparison of the calculated and the measured idler gain and NF spectra with two cascaded pump filters at 53.2 dB launched pump ESNR. A 0.95W pump power was used in calculation.

From the measurement results, both signal and idler NFs are above 5 dB, and can be up to more than 10 dB at the gain edges, which are actually not attractive for optical communication systems. To derive low NF, one can 1) use a low-noise pump laser (with < −160 dB/Hz RIN) and a low NF EDFA booster, 2) launch a low input signal power (well below −20 dBm) and 3) ensure relatively small signal-pump separation (far from the gain edges). Moreover, low-noise pump laser with high output power will be a good choice to replace the low power pump laser + EDFA scheme. By adopting the above modifications, the NF can reach 4 dB or even lower. Eventually the minimum achievable NF will be limited by the Raman phonon seeded noise [6]. In theory this thermal phonon induced noise limit can be reduced by cooling down the fiber [11], though it is impractical in real applications.

4. Conclusion

For the first time, the full signal and idler NF spectra of a single-pumped PI-FOPA have been achieved both theoretically and experimentally. Four main noise sources, which are amplified quantum noise, Raman phonon seeded excess noise, pump transferred noise and pump residual noise, respectively, are all accounted for. Measured results agree well with theory. Raman induced excess noise and Raman gain induced tilted PTN will both contribute to an asymmetric signal NF spectrum, however, the idler has a more symmetric NF spectrum.

Acknowledgement

This research leading to these results has received funding from the European Communities Seventh Framework Programme FP/2007-2013 under grant agreement 224547 (STREP PHASORS), and also from the Air Force Office of Scientific Research, Air Force Material Command, USAF, under grant number FA8655-09-1-3076. The U.S. Government is authorized to reproduce and distribute reprints for Governmental purpose notwithstanding any

copyright thereon. Z. Tong would like to thank Dr. Per-Olof Hedekvist for helping with error analysis, and Dr. Lars Grüner-Nielsen for providing the measurement data of the HNLF.

#118960 - $15.00 USD Received 26 Oct 2009; revised 10 Dec 2009; accepted 12 Jan 2010; published 27 Jan 2010